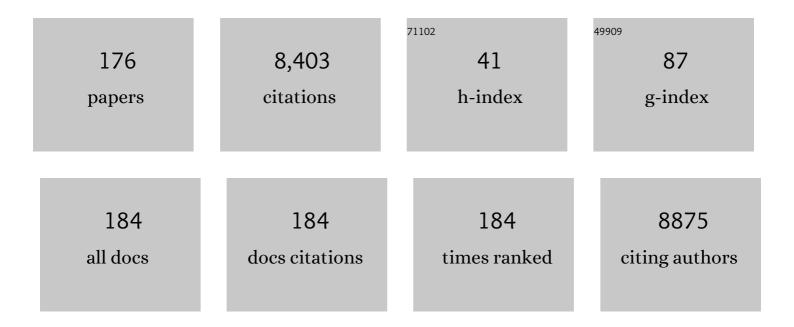
## Nikolaos Dikaios

List of Publications by Year in descending order

Source: https://exaly.com/author-pdf/2329741/publications.pdf Version: 2024-02-01



#	Article	IF	CITATIONS
1	MRI-Targeted or Standard Biopsy for Prostate-Cancer Diagnosis. New England Journal of Medicine, 2018, 378, 1767-1777.	27.0	2,036
2	Magnetic Resonance Imaging for the Detection, Localisation, and Characterisation of Prostate Cancer: Recommendations from a European Consensus Meeting. European Urology, 2011, 59, 477-494.	1.9	642
3	Standards of Reporting for MRI-targeted Biopsy Studies (START) of the Prostate: Recommendations from an International Working Group. European Urology, 2013, 64, 544-552.	1.9	383
4	STIR: software for tomographic image reconstruction release 2. Physics in Medicine and Biology, 2012, 57, 867-883.	3.0	375
5	Non-perforating small bowel Crohn's disease assessed by MRI enterography: Derivation and histopathological validation of an MR-based activity index. European Journal of Radiology, 2012, 81, 2080-2088.	2.6	234
6	Negative Predictive Value of Multiparametric Magnetic Resonance Imaging in the Detection of Clinically Significant Prostate Cancer in the Prostate Imaging Reporting and Data System Era: A Systematic Review and Meta-analysis. European Urology, 2020, 78, 402-414.	1.9	183
7	Diagnostic accuracy of magnetic resonance enterography and small bowel ultrasound for the extent and activity of newly diagnosed and relapsed Crohn's disease (METRIC): a multicentre trial. The Lancet Gastroenterology and Hepatology, 2018, 3, 548-558.	8.1	143
8	Microstructural Characterization of Normal and Malignant Human Prostate Tissue With Vascular, Extracellular, and Restricted Diffusion for Cytometry in Tumours Magnetic Resonance Imaging. Investigative Radiology, 2015, 50, 218-227.	6.2	137
9	<b>Pediatric and Adolescent Lymphoma:</b> Comparison of Whole-Body STIR Half-Fourier RARE MR Imaging with an Enhanced PET/CT Reference for Initial Staging <sup></sup> . Radiology, 2010, 255, 182-190.	7.3	132
10	Mural Crohn Disease: Correlation of Dynamic Contrast-enhanced MR Imaging Findings with Angiogenesis and Inflammation at Histologic Examination—Pilot Study. Radiology, 2009, 251, 369-379.	7.3	122
11	Quantified terminal ileal motility during MR enterography as a potential biomarker of Crohn's disease activity: a preliminary study. European Radiology, 2012, 22, 2494-2501.	4.5	119
12	Evaluation of Crohn's disease activity: Initial validation of a magnetic resonance enterography global score (MEGS) against faecal calprotectin. European Radiology, 2014, 24, 277-287.	4.5	110
13	Respiratory motion correction in dynamic MRI using robust data decomposition registration – Application to DCE-MRI. Medical Image Analysis, 2014, 18, 301-313.	11.6	109
14	Extracellular volume quantification by dynamic equilibrium cardiac computed tomography in cardiac amyloidosis. Journal of Cardiovascular Computed Tomography, 2015, 9, 585-592.	1.3	108
15	Dynamic MR Image Reconstruction–Separation From Undersampled (\${f k},t\$)-Space via Low-Rank Plus Sparse Prior. IEEE Transactions on Medical Imaging, 2014, 33, 1689-1701.	8.9	106
16	National implementation of multiâ€parametric magnetic resonance imaging for prostate cancer detection – recommendations from a <scp>UK</scp> consensus meeting. BJU International, 2018, 122, 13-25.	2.5	106
17	Quantitative assessment of small bowel motility by nonrigid registration of dynamic MR images. Magnetic Resonance in Medicine, 2012, 68, 783-793.	3.0	97
18	Five-year Outcomes of Magnetic Resonance Imaging–based Active Surveillance for Prostate Cancer: A Large Cohort Study. European Urology, 2020, 78, 443-451.	1.9	94

#	Article	IF	CITATIONS
19	The PICTURE study: diagnostic accuracy of multiparametric MRI in men requiring a repeat prostate biopsy. British Journal of Cancer, 2017, 116, 1159-1165.	6.4	90
20	MRI-based motion correction of thoracic PET: initial comparison of acquisition protocols and correction strategies suitable for simultaneous PET/MRI systems. European Radiology, 2012, 22, 439-446.	4.5	82
21	Diffusion-weighted MRI of lymphoma: prognostic utility and implications for PET/MRI?. European Journal of Nuclear Medicine and Molecular Imaging, 2013, 40, 373-385.	6.4	77
22	"Textural analysis of multiparametric MRI detects transition zone prostate cancer― European Radiology, 2017, 27, 2348-2358.	4.5	74
23	Temporal and anatomical variations of brain water apparent diffusion coefficient in perinatal cerebral hypoxic-ischemic injury: Relationships to cerebral energy metabolism. Magnetic Resonance in Medicine, 1998, 39, 920-927.	3.0	73
24	UK quantitative WB-DWI technical workgroup: consensus meeting recommendations on optimisation, quality control, processing and analysis of quantitative whole-body diffusion-weighted imaging for cancer. British Journal of Radiology, 2018, 91, 20170577.	2.2	70
25	Diffusion weighted imaging of female pelvic cancers: Concepts and clinical applications. European Journal of Radiology, 2011, 78, 21-29.	2.6	69
26	The SmartTarget Biopsy Trial: A Prospective, Within-person Randomised, Blinded Trial Comparing the Accuracy of Visual-registration and Magnetic Resonance Imaging/Ultrasound Image-fusion Targeted Biopsies for Prostate Cancer Risk Stratification. European Urology, 2019, 75, 733-740.	1.9	67
27	Whole-body MRI quantitative biomarkers are associated significantly with treatment response in patients with newly diagnosed symptomatic multiple myeloma following bortezomib induction. European Radiology, 2017, 27, 5325-5336.	4.5	62
28	What Type of Prostate Cancer Is Systematically Overlooked by Multiparametric Magnetic Resonance Imaging? An Analysis from the PROMIS Cohort. European Urology, 2020, 78, 163-170.	1.9	60
29	Multiparametric MRI for detection of radiorecurrent prostate cancer: added value of apparent diffusion coefficient maps and dynamic contrast-enhanced images. Prostate Cancer and Prostatic Diseases, 2015, 18, 128-136.	3.9	59
30	Impact of <sup>68</sup> Ga-Prostate-Specific Membrane Antigen PET/CT on Prostate Cancer Management. Journal of Nuclear Medicine, 2018, 59, 89-92.	5.0	58
31	Patient Reported Outcome Measures for Transperineal Template Prostate Mapping Biopsies in the PICTURE Study. Journal of Urology, 2018, 200, 1235-1240.	0.4	55
32	Machine learning classifiers can predict Gleason pattern 4 prostate cancer with greater accuracy than experienced radiologists. European Radiology, 2019, 29, 4754-4764.	4.5	55
33	The effect of low resolution and coverage on the accuracy of susceptibility mapping. Magnetic Resonance in Medicine, 2019, 81, 1833-1848.	3.0	53
34	Mathematical models and deep learning for predicting the number of individuals reported to be infected with SARS-CoV-2. Journal of the Royal Society Interface, 2020, 17, 20200494.	3.4	53
35	VERDICT MRI for Prostate Cancer: Intracellular Volume Fraction versus Apparent Diffusion Coefficient. Radiology, 2019, 291, 391-397.	7.3	52
36	Diagnostic accuracy of whole-body MRI versus standard imaging pathways for metastatic disease in newly diagnosed colorectal cancer: the prospective Streamline C trial. The Lancet Gastroenterology and Hepatology, 2019, 4, 529-537.	8.1	51

#	Article	IF	CITATIONS
37	The PICTURE study — Prostate Imaging (multi-parametric MRI and Prostate HistoScanning™) Compared to Transperineal Ultrasound guided biopsy for significant prostate cancer Risk Evaluation. Contemporary Clinical Trials, 2014, 37, 69-83.	1.8	50
38	Diagnostic accuracy of whole-body MRI versus standard imaging pathways for metastatic disease in newly diagnosed non-small-cell lung cancer: the prospective Streamline L trial. Lancet Respiratory Medicine,the, 2019, 7, 523-532.	10.7	50
39	Whole body magnetic resonance imaging in newly diagnosed multiple myeloma: early changes in lesional signal fat fraction predict disease response. British Journal of Haematology, 2017, 176, 222-233.	2.5	48
40	Simultaneous Quantification of Bone Edema/Adiposity and Structure in Inflamed Bone Using Chemical Shiftâ€Encoded <scp>MRI</scp> in Spondyloarthritis. Magnetic Resonance in Medicine, 2018, 79, 1031-1042.	3.0	47
41	Photoacoustic imaging of human lymph nodes with endogenous lipid and hemoglobin contrast. Journal of Biomedical Optics, 2015, 20, 1.	2.6	45
42	Understanding PI-QUAL for prostate MRI quality: a practical primer for radiologists. Insights Into Imaging, 2021, 12, 59.	3.4	43
43	Comparative evaluation of two commercial PET scanners, ECAT EXACT HR+ and Biograph 2, using GATE. Nuclear Instruments and Methods in Physics Research, Section A: Accelerators, Spectrometers, Detectors and Associated Equipment, 2006, 569, 368-372.	1.6	41
44	Logistic regression model for diagnosis of transition zone prostate cancer on multi-parametric MRI. European Radiology, 2015, 25, 523-532.	4.5	40
45	INNOVATE: A prospective cohort study combining serum and urinary biomarkers with novel diffusion-weighted magnetic resonance imaging for the prediction and characterization of prostate cancer. BMC Cancer, 2016, 16, 816.	2.6	40
46	Fat fraction mapping using magnetic resonance imaging: insight into pathophysiology. British Journal of Radiology, 2018, 91, 20170344.	2.2	39
47	Diagnostic utility of whole body Dixon MRI in multiple myeloma: A multi-reader study. PLoS ONE, 2017, 12, e0180562.	2.5	38
48	Accuracy of Transperineal Targeted Prostate Biopsies, Visual Estimation and Image Fusion in Men Needing Repeat Biopsy in the PICTURE Trial. Journal of Urology, 2018, 200, 1227-1234.	0.4	38
49	Natural history of prostate cancer on active surveillance: stratification by MRI using the PRECISE recommendations in a UK cohort. European Radiology, 2021, 31, 1644-1655.	4.5	37
50	Quantitative diffusion weighted MRI: A functional biomarker of nodal disease in Hodgkin lymphoma?. Cancer Biomarkers, 2011, 7, 249-259.	1.7	36
51	Automatic quantification of the myocardial extracellular volume by cardiac computed tomography: Synthetic ECV by CCT. Journal of Cardiovascular Computed Tomography, 2017, 11, 221-226.	1.3	34
52	Multiparametric whole-body 3.0-T MRI in newly diagnosed intermediate- and high-risk prostate cancer: diagnostic accuracy and interobserver agreement for nodal and metastatic staging. European Radiology, 2019, 29, 3159-3169.	4.5	34
53	Whole-body MRI compared with standard pathways for staging metastatic disease in lung and colorectal cancer: the Streamline diagnostic accuracy studies. Health Technology Assessment, 2019, 23, 1-270.	2.8	34
54	Direct parametric reconstruction from undersampled (k, t)-space data in dynamic contrast enhanced MRI. Medical Image Analysis, 2014, 18, 989-1001.	11.6	33

#	Article	IF	CITATIONS
55	An optimized and highly repeatable MRI acquisition and processing pipeline for quantitative susceptibility mapping in the headâ€andâ€neck region. Magnetic Resonance in Medicine, 2020, 84, 3206-3222.	3.0	33
56	Certification in reporting multiparametric magnetic resonance imaging of the prostate: recommendations of a UK consensus meeting. BJU International, 2021, 127, 304-306.	2.5	32
57	Inter-reader agreement of the PI-QUAL score for prostate MRI quality in the NeuroSAFE PROOF trial. European Radiology, 2022, 32, 879-889.	4.5	32
58	Artificial Intelligence Compared to Radiologists for the Initial Diagnosis of Prostate Cancer on Magnetic Resonance Imaging: A Systematic Review and Recommendations for Future Studies. Cancers, 2021, 13, 3318.	3.7	32
59	Zone-specific logistic regression models improve classification of prostate cancer on multi-parametric MRI. European Radiology, 2015, 25, 2727-2737.	4.5	29
60	Whole-body MRI for staging and interim response monitoring in paediatric and adolescent Hodgkin's lymphoma: a comparison with multi-modality reference standard including 18F-FDG-PET-CT. European Radiology, 2019, 29, 202-212.	4.5	29
61	Noninvasive diffusion magnetic resonance imaging of brain tumour cell size for the early detection of therapeutic response. Scientific Reports, 2020, 10, 9223.	3.3	29
62	A Multicentre Analysis of the Detection of Clinically Significant Prostate Cancer Following Transperineal Image-fusion Targeted and Nontargeted Systematic Prostate Biopsy in Men at Risk. European Urology Oncology, 2020, 3, 262-269. In predict upgrading of transrectal ultrasound biopsy.	5.4	28
63	results at more definitive histology?11Mohamed Abd-Alazeez receives funding from the Egyptian government. Mark Emberton and Hashim U. Ahmed receive funding from USHIFU and Advanced Medical Diagnostics for clinical trials. Mark Emberton is a paid consultant for Steba Biotech, USHIFU and Sanofi-Aventis. Mark Emberton has received research support by GSK for a study evaluating the role of	1.6	27
64	MRI in men with prostate. Urologic Oncology: Seminars and Original Investigations, 2014, 32, 741-747. Apparatus for Histological Validation of In Vivo and Ex Vivo Magnetic Resonance Imaging of the Human Prostate. Frontiers in Oncology, 2017, 7, 47.	2.8	27
65	Additional Value of Dynamic Contrast-enhanced Sequences in Multiparametric Prostate Magnetic Resonance Imaging: Data from the PROMIS Study. European Urology, 2020, 78, 503-511.	1.9	27
66	Noise estimation from averaged diffusion weighted images: Can unbiased quantitative decay parameters assist cancer evaluation?. Magnetic Resonance in Medicine, 2014, 71, 2105-2117.	3.0	25
67	Characterizing indeterminate (Likert-score 3/5) peripheral zone prostate lesions with PSA density, PI-RADS scoring and qualitative descriptors on multiparametric MRI. British Journal of Radiology, 2018, 91, 20170645.	2.2	23
68	VERDICT MRI validation in fresh and fixed prostate specimens using patientâ€specific moulds for histological and MR alignment. NMR in Biomedicine, 2019, 32, e4073.	2.8	22
69	Prostate MRI quality: a critical review of the last 5 years and the role of the PI-QUAL score. British Journal of Radiology, 2022, 95, 20210415.	2.2	22
70	Changes in dynamic contrast-enhanced pharmacokinetic and diffusion-weighted imaging parameters reflect response to anti-TNF therapy in Crohn's disease. British Journal of Radiology, 2015, 88, 20150547.	2.2	21
71	Streamlining staging of lung and colorectal cancer with whole body MRI; study protocols for two multicentre, non-randomised, single-arm, prospective diagnostic accuracy studies (Streamline C and) Tj ETQq1 1	0. <b>2&amp;</b> 4314	rgBT /Overl
72	Contrast enhanced MR imaging of female pelvic cancers: Established methods and emerging applications. European Journal of Radiology, 2011, 78, 2-11.	2.6	20

#	Article	IF	CITATIONS
73	Interobserver reproducibility of the PRECISE scoring system for prostate MRI on active surveillance: results from a two-centre pilot study. European Radiology, 2020, 30, 2082-2090.	4.5	20
74	A few-shot U-Net deep learning model for lung cancer lesion segmentation via PET/CT imaging. Biomedical Physics and Engineering Express, 2022, 8, 025019.	1.2	20
75	VERDICTâ€AMICO: Ultrafast fitting algorithm for nonâ€invasive prostate microstructure characterization. NMR in Biomedicine, 2019, 32, e4019.	2.8	19
76	Computer-aided diagnosis of prostate cancer using multiparametric MRI and clinical features: A patient-level classification framework. Medical Image Analysis, 2021, 73, 102153.	11.6	19
77	Dynamic contrast-enhanced MRI improves accuracy for detecting focal splenic involvement in children and adolescents with Hodgkin disease. Pediatric Radiology, 2013, 43, 941-949.	2.0	18
78	Evolution of multi-parametric MRI quantitative parameters following transrectal ultrasound-guided biopsy of the prostate. Prostate Cancer and Prostatic Diseases, 2015, 18, 343-351.	3.9	18
79	Feasibility of vocal fold abduction and adduction assessment using cine-MRI. European Radiology, 2017, 27, 598-606.	4.5	18
80	A comparison of Bayesian and non-linear regression methods for robust estimation of pharmacokinetics in DCE-MRI and how it affects cancer diagnosis. Computerized Medical Imaging and Graphics, 2017, 56, 1-10.	5.8	18
81	Prediction of Pediatric Percutaneous Nephrolithotomy Outcomes Using Contemporary Scoring Systems. Journal of Urology, 2017, 198, 1146-1152.	0.4	18
82	GAS: A genetic atlas selection strategy in multi-atlas segmentation framework. Medical Image Analysis, 2019, 52, 97-108.	11.6	18
83	Update on Multiparametric Prostate MRI During Active Surveillance: Current and Future Trends and Role of the PRECISE Recommendations. American Journal of Roentgenology, 2021, 216, 943-951.	2.2	18
84	Harnessing Uncertainty in Domain Adaptation for MRI Prostate Lesion Segmentation. Lecture Notes in Computer Science, 2020, , 510-520.	1.3	17
85	Paediatric CT: the effects of increasing image noise on pulmonary nodule detection. Pediatric Radiology, 2008, 38, 192-201.	2.0	16
86	Improved motionâ€compensated image reconstruction for PET using sensitivity correction per respiratory gate and an approximate tubeâ€ofâ€response backprojector. Medical Physics, 2011, 38, 4958-4970.	3.0	16
87	Simplified Luminal Water Imaging for the Detection of Prostate Cancer From Multiecho T <sub>2</sub> MR Images. Journal of Magnetic Resonance Imaging, 2019, 50, 910-917.	3.4	16
88	A Dedicated Prostate MRI Teaching Course Improves the Ability of the Urologist to Interpret Clinically Significant Prostate Cancer on Multiparametric MRI. European Urology, 2019, 75, 203-204.	1.9	16
89	Acceleration of motion-compensated PET reconstruction: ordered subsets-gates EM algorithms and <i>a priori</i> reference gate information. Physics in Medicine and Biology, 2011, 56, 1695-1715.	3.0	15
90	<sup>18</sup> F-FDG PET/MRI for Staging and Interim Response Assessment in Pediatric and Adolescent Hodgkin Lymphoma: A Prospective Study with <sup>18</sup> F-FDG PET/CT as the Reference Standard. Journal of Nuclear Medicine, 2021, 62, 1524-1530.	5.0	15

#	Article	IF	CITATIONS
91	A multicentre randomised controlled trial assessing whether MRI-targeted biopsy is non-inferior to standard transrectal ultrasound guided biopsy for the diagnosis of clinically significant prostate cancer in men without prior biopsy: a study protocol. BMJ Open, 2017, 7, e017863.	1.9	14
92	Optimization and repeatability of multipool chemical exchange saturation transfer MRI of the prostate at 3.0 T. Journal of Magnetic Resonance Imaging, 2019, 50, 1238-1250.	3.4	14
93	DWI and PRECISE criteria in men on active surveillance for prostate cancer: A multicentre preliminary experience of different ADC calculations. Magnetic Resonance Imaging, 2020, 67, 50-58.	1.8	14
94	The natural history of prostate cancer on MRI: lessons from an active surveillance cohort. Prostate Cancer and Prostatic Diseases, 2018, 21, 556-563.	3.9	13
95	Prediction of significant prostate cancer in biopsy-naÃ <sup>-</sup> ve men: Validation of a novel risk model combining MRI and clinical parameters and comparison to an ERSPC risk calculator and PI-RADS. PLoS ONE, 2019, 14, e0221350.	2.5	13
96	Targeted biopsy of the prostate: does this result in improvement in detection of highâ€grade cancer or the occurrence of the Will Rogers phenomenon?. BJU International, 2019, 124, 643-648.	2.5	13
97	Prostate cancer treated with irreversible electroporation: MRI-based volumetric analysis and oncological outcome. Magnetic Resonance Imaging, 2019, 58, 143-147.	1.8	13
98	Sequential prostate MRI reporting in men on active surveillance: initial experience of a dedicated PRECISE software program. Magnetic Resonance Imaging, 2019, 57, 34-39.	1.8	13
99	False Positive Multiparametric Magnetic Resonance Imaging Phenotypes in the Biopsy-naÃ <sup>-</sup> ve Prostate: Are They Distinct from Significant Cancer-associated Lesions? Lessons from PROMIS. European Urology, 2021, 79, 20-29.	1.9	13
100	Estimation of contrast agent bolus arrival delays for improved reproducibility of liver DCE MRI. Physics in Medicine and Biology, 2016, 61, 6905-6918.	3.0	12
101	Statistical limitations in proton imaging. Physics in Medicine and Biology, 2020, 65, 085011.	3.0	12
102	OCTAVA: An open-source toolbox for quantitative analysis of optical coherence tomography angiography images. PLoS ONE, 2021, 16, e0261052.	2.5	12
103	Prostate cancer measurements on serial MRI during active surveillance: it's time to be PRECISE. British Journal of Radiology, 2020, 93, 20200819.	2.2	11
104	An end-to-end assessment on the accuracy of adaptive radiotherapy in an MR-linac. Physics in Medicine and Biology, 2021, 66, 055021.	3.0	11
105	Standardisation of prostate multiparametric MRI across a hospital network: a London experience. Insights Into Imaging, 2021, 12, 52.	3.4	11
106	Scatter Simulation Including Double Scatter. , 0, , .		10
107	Association of bone mineral density and fat fraction with magnetic susceptibility in inflamed trabecular bone. Magnetic Resonance in Medicine, 2019, 81, 3094-3107.	3.0	10
108	Evaluation of PSA and PSA Density in a Multiparametric Magnetic Resonance Imaging-Directed Diagnostic Pathway for Suspected Prostate Cancer: The INNOVATE Trial. Cancers, 2021, 13, 1985.	3.7	10

#	Article	IF	CITATIONS
109	ReIMAGINE Prostate Cancer Screening Study: protocol for a single-centre feasibility study inviting men for prostate cancer screening using MRI. BMJ Open, 2021, 11, e048144.	1.9	10
110	AutoProstate: Towards Automated Reporting of Prostate MRI for Prostate Cancer Assessment Using Deep Learning. Cancers, 2021, 13, 6138.	3.7	10
111	Registration-weighted motion correction for PET. Medical Physics, 2012, 39, 1253-1264.	3.0	9
112	Immunohistochemical biomarker validation in highly selective needle biopsy microarrays derived from mpMRl haracterized prostates. Prostate, 2018, 78, 1229-1237.	2.3	9
113	Localising occult prostate cancer metastasis with advanced imaging techniques (LOCATE trial): a prospective cohort, observational diagnostic accuracy trial investigating whole–body magnetic resonance imaging in radio-recurrent prostate cancer. BMC Medical Imaging, 2019, 19, 90.	2.7	9
114	Management of Radiologically Indeterminate Magnetic Resonance Imaging Signals in Men at Risk of Prostate Cancer. European Urology Focus, 2019, 5, 62-68.	3.1	9
115	Comparison of Transrectal Ultrasound Biopsy to Transperineal Template Mapping Biopsies Stratified by Multiparametric Magnetic Resonance Imaging Score in the PROMIS Trial. Journal of Urology, 2020, 203, 100-107.	0.4	9
116	Magnetic Resonance Imaging and Targeted Biopsies Compared to Transperineal Mapping Biopsies Before Focal Ablation in Localised and Metastatic Recurrent Prostate Cancer After Radiotherapy. European Urology, 2022, 81, 598-605.	1.9	9
117	Multi-parametric MRI zone-specific diagnostic model performance compared with experienced radiologists for detection of prostate cancer. European Radiology, 2019, 29, 4150-4159.	4.5	8
118	Added value of diffusionâ€weighted images and dynamic contrast enhancement in multiparametric magnetic resonance imaging for the detection of clinically significant prostate cancer in the PICTURE trial. BJU International, 2020, 125, 391-398.	2.5	8
119	Stochastic Gradient Langevin dynamics for joint parameterization of tracer kinetic models, input functions, and T1 relaxation-times from undersampled k-space DCE-MRI. Medical Image Analysis, 2020, 62, 101690.	11.6	8
120	Whole body MRI in multiple myeloma: Optimising image acquisition and read times. PLoS ONE, 2020, 15, e0228424.	2.5	8
121	Imageâ€Guided Magnetic Thermoseed Navigation and Tumor Ablation Using a Magnetic Resonance Imaging System. Advanced Science, 2022, , 2105333.	11.2	8
122	Prostate Cancer Classification on VERDICT DW-MRI Using Convolutional Neural Networks. Lecture Notes in Computer Science, 2018, , 319-327.	1.3	7
123	Deep learning magnetic resonance spectroscopy fingerprints of brain tumours using quantum mechanically synthesised data. NMR in Biomedicine, 2021, 34, e4479.	2.8	7
124	Covid-19: predictive mathematical formulae for the number of deaths during lockdown and possible scenarios for the post-lockdown period. Proceedings of the Royal Society A: Mathematical, Physical and Engineering Sciences, 2021, 477, 20200745.	2.1	7
125	Improved hepatic arterial fraction estimation using cardiac output correction of arterial input functions for liver DCE MRI. Physics in Medicine and Biology, 2017, 62, 1533-1546.	3.0	6
126	Long-term biopsy outcomes in prostate cancer patients treated with external beam radiotherapy: a systematic review and meta-analysis. Prostate Cancer and Prostatic Diseases, 2021, 24, 612-622.	3.9	6

#	Article	IF	CITATIONS
127	Statistical limitations in ion imaging. Physics in Medicine and Biology, 2021, 66, 105009.	3.0	6
128	Can We Improve the Reproducibility of Quantitative Multiparametric Prostate MR Imaging Metrics?. Radiology, 2016, 281, 652-653.	7.3	5
129	Whole Body 3.0 T Magnetic Resonance Imaging in Lymphomas: Comparison of Different Sequence Combinations for Staging Hodgkin's and Diffuse Large B Cell Lymphomas. Journal of Personalized Medicine, 2020, 10, 284.	2.5	5
130	Texture Analysis of Fractional Water Content Images Acquired during PET/MRI: Initial Evidence for an Association with Total Lesion Glycolysis, Survival and Gene Mutation Profile in Primary Colorectal Cancer. Cancers, 2021, 13, 2715.	3.7	5
131	Update from the ReIMAGINE Prostate Cancer Screening Study NCT04063566: Inviting Men for Prostate Cancer Screening Using Magnetic Resonance Imaging. European Urology Focus, 2021, 7, 503-505.	3.1	5
132	Tumour growth rates of prostate cancer during active surveillance: is there a difference between MRI-visible low and intermediate-risk disease?. British Journal of Radiology, 2022, 95, 20210321.	2.2	5
133	Emerging methods for prostate cancer imaging: evaluating cancer structure and metabolic alterations more clearly. Molecular Oncology, 2021, 15, 2565-2579.	4.6	5
134	Diagnostic Accuracy of Abbreviated Bi-Parametric MRI (a-bpMRI) for Prostate Cancer Detection and Screening: A Multi-Reader Study. Diagnostics, 2022, 12, 231.	2.6	5
135	Whole-body magnetic resonance imaging in paediatric Hodgkin lymphoma — evaluation of quantitative magnetic resonance metrics for nodal staging. Pediatric Radiology, 2019, 49, 1285-1298.	2.0	4
136	A critical evaluation of visual proportion of Gleason 4 and maximum cancer core length quantified by histopathologists. Scientific Reports, 2020, 10, 17177.	3.3	4
137	Synthetic Q-Space Learning With Deep Regression Networks For Prostate Cancer Characterisation With Verdict. , 2021, , .		4
138	Respiratory Motion Correction in Dynamic-MRI: Application to Small Bowel Motility Quantification during Free Breathing. Lecture Notes in Computer Science, 2013, 16, 132-140.	1.3	4
139	Double Scatter Simulation using the Polarized Klein-Nishina formula. , 2006, , .		3
140	A Probabilistic Method for Estimation of Bowel Wall Thickness in MR Colonography. PLoS ONE, 2017, 12, e0168317.	2.5	3
141	Reconstruction of Preclinical PET Images via Chebyshev Polynomial Approximation of the Sinogram. Applied Sciences (Switzerland), 2022, 12, 3335.	2.5	3
142	Processing of transmission data from an uncollimated single photon source. Nuclear Instruments and Methods in Physics Research, Section A: Accelerators, Spectrometers, Detectors and Associated Equipment, 2006, 569, 416-420.	1.6	2
143	Respiratory motion correction of PET using motion parameters from MR. , 2009, , .		2
144	Initial validation of equilibrium contrast imaging for extracellular volume quantification using a threeâ€dimensional engineered tissue model. Journal of Magnetic Resonance Imaging, 2016, 43, 1224-1229.	3.4	2

#	Article	IF	CITATIONS
145	Machine learning for proton path tracking in proton computed tomography. Physics in Medicine and Biology, 2021, 66, 105013.	3.0	2
146	Quantification of T1, T2 relaxation times from Magnetic Resonance Fingerprinting radially undersampled data using analytical transformations. Magnetic Resonance Imaging, 2021, 80, 81-89.	1.8	2
147	Unsupervised Domain Adaptation with Semantic Consistency Across Heterogeneous Modalities for MRI Prostate Lesion Segmentation. Lecture Notes in Computer Science, 2021, , 90-100.	1.3	2
148	Feasibility of Data-Driven, Model-Free Quantitative MRI Protocol Design: Application to Brain and Prostate Diffusion-Relaxation Imaging. Frontiers in Physics, 2021, 9, .	2.1	2
149	The ReIMAGINE Multimodal Warehouse: Using Artificial Intelligence for Accurate Risk Stratification of Prostate Cancer. Frontiers in Artificial Intelligence, 2021, 4, 769582.	3.4	2
150	Discrete Shearlets as a Sparsifying Transform in Low-Rank Plus Sparse Decomposition for Undersampled (k, t)-Space MR Data. Journal of Imaging, 2022, 8, 29.	3.0	2
151	The ReIMAGINE prostate cancer risk study protocol: A prospective cohort study in men with a suspicion of prostate cancer who are referred onto an MRI-based diagnostic pathway with donation of tissue, blood and urine for biomarker analyses PLoS ONE, 2022, 17, e0259672.	2.5	2
152	A reproducible dynamic phantom for sequence testing in hyperpolarised <sup>13</sup> C-magnetic resonance. British Journal of Radiology, 2022, 95, 20210770.	2.2	2
153	Joint reconstruction of low-rank and sparse components from undersampled (k, t)-space small bowel data. , 2013, , .		1
154	Synthesizing VERDICT Maps from Standard DWI Data Using GANs. Lecture Notes in Computer Science, 2021, , 58-67.	1.3	1
155	Molière maximum likelihood proton path estimation approximated by cubic Bézier curve for scatter corrected proton CT reconstruction. Physics in Medicine and Biology, 2020, 65, 175003.	3.0	1
156	Whole Body (WB) MRI in Newly Diagnosed Multiple Myeloma (MM): Fat Fraction Changes at 8 Weeks Predict Response to Induction with Bortezomib Regimens. Blood, 2015, 126, 1850-1850.	1.4	1
157	Simple Formulae, Deep Learning and Elaborate Modelling for the COVID-19 Pandemic. Encyclopedia, 2022, 2, 679-689.	4.5	1
158	Multi-scale analysis of apparent diffusion coefficient (ADC) predicts cervical nodal status in patients with head and neck squamous cell carcinoma. British Journal of Oral and Maxillofacial Surgery, 2013, 51, e81.	0.8	0
159	Direct parametric reconstruction from undersampled (k, t)-space data in dynamic contrast enhancement MRI. , 2013, , .		0
160	Multi-modal pharmacokinetic modelling for DCE-MRI: using diffusion weighted imaging to constrain the local arterial input function. Proceedings of SPIE, 2014, , .	0.8	0
161	MP53-05 MULTI-PARAMETRIC MRI FOR DETECTION OF RADIO-RECURRENT PROSTATE CANCER: WHAT CONSTITUTES AN OPTIMAL DATASET?. Journal of Urology, 2014, 191, .	0.4	0
162	VERDICT Prostate Parameter Estimation with AMICO. Mathematics and Visualization, 2018, , 229-241.	0.6	0

#	Article	IF	CITATIONS
163	Integration of Proton Computed Tomography into the Open Source Software STIR. , 2019, , .		0
164	Proton Computed Tomography: A Case Study for Optimal Data Acquisition. , 2019, , .		0
165	Followup of Men with PI-RADS TM 4 or 5 Abnormality on Prostate Magnetic Resonance Imaging and Nonmalignant Pathological Findings on Initial Targeted Prostate Biopsy. Letter Journal of Urology, 2021, 205, 1526-1528.	0.4	0
166	Utility of diffusion MRI characteristics of cervical lymph nodes as disease classifier between patients with head and neck squamous cell carcinoma and healthy volunteers. NMR in Biomedicine, 2021, 34, e4587.	2.8	0
167	PO-1667 Statistical limitations in particle imaging tomography. Radiotherapy and Oncology, 2021, 161, S1390-S1391.	0.6	Ο
168	Sparse-Input Neural Networks to Differentiate 32 Primary Cancer Types on the Basis of Somatic Point Mutations. Onco, 2022, 2, 56-68.	0.6	0
169	Histo-MRI map study protocol: a prospective cohort study mapping MRI to histology for biomarker validation and prediction of prostate cancer. BMJ Open, 2022, 12, e059847.	1.9	0
170	Whole body MRI in multiple myeloma: Optimising image acquisition and read times. , 2020, 15, e0228424.		0
171	Whole body MRI in multiple myeloma: Optimising image acquisition and read times. , 2020, 15, e0228424.		0
172	Whole body MRI in multiple myeloma: Optimising image acquisition and read times. , 2020, 15, e0228424.		0
173	Whole body MRI in multiple myeloma: Optimising image acquisition and read times. , 2020, 15, e0228424.		0
174	MO-0218 A likelihood-based particle imaging filter using prior information. Radiotherapy and Oncology, 2022, 170, S175-S176.	0.6	0
175	Cross-Modality Image Registration Using a Training-Time Privileged Third Modality. IEEE Transactions on Medical Imaging, 2022, 41, 3421-3431.	8.9	Ο
176	Differentiating False Positive Lesions from Clinically Significant Cancer and Normal Prostate Tissue Using VERDICT MRI and Other Diffusion Models. Diagnostics, 2022, 12, 1631.	2.6	0